The Photogrammetric Record 24(128): 372–385 (December 2009)

Shorter Contribution

THE BUILDING SHADOW PROBLEM OF AIRBORNE LIDAR

PETER TIAN-YUAN SHIH (tyshih@mail.nctu.edu.tw)
National Chiao Tung University, Hsinchu, Taiwan

CHING-MEI HUANG (candice@ceci.com.tw)
CECI Engineering Consultants Inc., Taipei, Taiwan

Abstract

Airborne lidar systems are equipped with a scanning mechanism that produces a swath of 3D coordinated points to form a cloud in each flight strip. The scanning is perpendicular to the direction of flight. The density of the point cloud is one of the major quality measures for the data collected with such systems. Point density, shade (occlusion of the laser beam) and penetration rate are major factors to be considered in the flight design. For practical operations, flight missions may be designed with overlaps ranging from 5 to 50%. Aside from the percentage overlap, the field of view is another important parameter for flight design. An evaluation scheme to assess the percentage overlap between flight strips and the selection of the field of view is proposed in this study. The influences of overlap and field of view are also demonstrated with real data gathered by an airborne lidar system.

KEYWORDS: airborne laser scanning, digital elevation model, field of view, flight planning, laser shadow, lidar, percentage overlap

INTRODUCTION

THE SYSTEM OF AIRBORNE LIDAR, also known as airborne laser scanning, is equipped with a scanning mechanism which produces a swath of 3D coordinated points to form a point cloud in each flight strip (Ackermann, 1999; Baltsavias, 1999). The scanning is performed perpendicular to the path of the aircraft (''across-track''). While the frequency of the scan line is generally about 200 lines per second, the repetition rate of the laser subsystem can reach 100 kHz or above. After the raw point cloud data is collected, which includes the returns from both the terrain itself and material above the terrain, such as trees and other vegetation, a filtering and editing process (such as that proposed by Sohn and Dowman, 2008) is required to separate the terrain points from the rest, in order to construct the digital elevation model (DEM) for topographic mapping. There also exist applications other than topographic mapping, such as volume estimation for forestry (Lim et al., 2003; van Aardt, 2004) and building model generation (Zhang et al., 2005). But, no matter what the application or how complex the method of processing, the density of the point clouds is one of the major quality measures for

the data collected with airborne lidar. Point density, shade (or occlusion) effects and penetration rate are the major factors considered in flight design.

The completeness of coverage, the density and the even distribution of points are major concerns for an airborne lidar project. All these are highly related to the swath overlap in the flight design. In a practical operation, missions may be designed with overlap ranging from 5 to 50%. If the flying height above the terrain can be maintained in a stable manner, 5% overlap could be sufficient for avoiding gaps between strips. The US National Geodetic Survey requires at least 25% overlap for shoreline mapping applications and at least 50% overlap for airport surveying (NGS, 2004a, b, respectively). The contribution of high percentage overlap not only reduces the risk of gaps, but also improves the point density. From the block adjustment point of view, higher percentage overlap can also strengthen the geometric configuration.

Besides the percentage overlap, field of view (FOV) is another important parameter of flight design. Both are directly related to the surface obstruction. The surface obstruction error is well documented in James et al. (2006). An image processing scheme with optical supporting imagery is proposed for removing obstruction error. The distribution and ratio of shade is also a characteristic of different vegetation ecosystems. Varga and Asner (2008) made use of bare substrate and shade ratio for fire fuel studies. It is well known that the larger the overlap, the higher the density, and the smaller the FOV, the better the penetration rate. However, the trade-offs are the longer period of operation and higher financial cost required. An evaluation scheme to assess the percentage overlap between flight strips and the selection of FOV is proposed in this study. The influences of overlap and FOV are also demonstrated with data gathered by a Leica ALS50 airborne lidar system.

Point Density Variation Across Strip

In the coverage of a single strip, the lidar points are not evenly distributed because the scan direction is perpendicular to the direction of flight and the oscillating mirror, such as the one used in the Leica ALS50, generates a zigzag scanning pattern on the ground. This scanning mechanism causes uneven speed in each scan line. The central portion of the scan line has the highest scan speed and the speed at the two edges is essentially zero. Unlike the sophisticated design used for bathymetric lidar, which provides equal spacing of points across a strip (Guenther et al., 1996; Sinclair, 2005), the scanning mechanism implemented with airborne lidar designed for mapping of land areas does not compensate for this issue. As a result, along the scan line, the point densities along the two sides are higher, and the density is lower near the strip centre, as shown in Fig. 1.

Such phenomena can be illustrated by examining the raw point cloud data collected on a practical mission carried out in Fu-Hsing-Tou, Hsinchu, Taiwan. As shown in Table I, three strips were divided into five sub-strips each. The ground width of each sub-strip is the same. The uneven point distribution of all three strips displayed the same pattern. Although there are

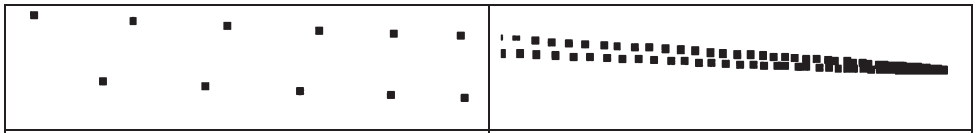

Fig. 1. Point density variation along a scan line.

TABLE I. Numbers of lidar points in the raw point clouds, Fu-Hsing-Tou, Hsinchu.

Strip	*Left2*	*Left1*	*Centre*	*Right1*	*Right2*
26	786923	429898	396761	424894	801625
27	799650	424174	388710	423279	815088
28	795386	417381	383423	402695	828266

many other factors, such as the ground cover type, the scanning mechanism is considered one of the main factors.

SHADING FROM THE OBJECT

Objects on top of the terrain, as well as the undulations of the terrain itself, may cause shadows (occlusions of the laser beam). That is, the laser beam would not reach a ground area on the opposite side of the object from the sensor. Taking a building as an example, Fig. 2 illustrates the relationship between the angle of incidence, the height of the building and the location of the laser origin. The grey area in Fig. 2 represents the shadow caused by the building.

The length of shadow is related to several geometric parameters. This can be described by the following equation:

$$c = \frac{h_b l}{H - h_b}. \tag{1}$$

The parameters in Fig. 2 represent:

H: flying height above the terrain
h_b: height of the building
c: length of the shadow
l: horizontal distance between the building and the laser origin.

From equation (1), the length of shadow c can be calculated from H, h_b and l. Table II lists the numerical value of shadow lengths for some combinations.

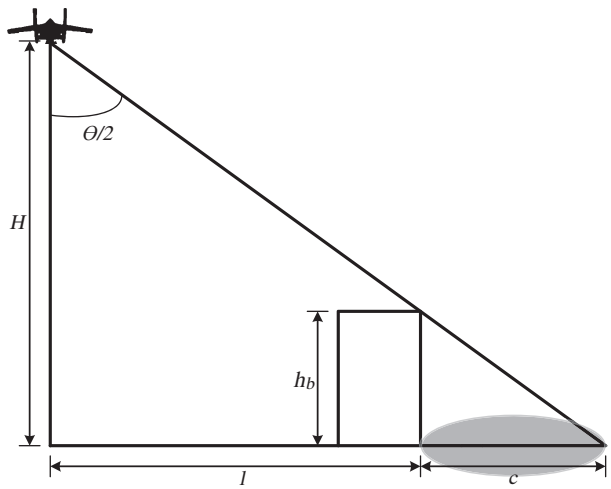

FIG. 2. Building shadow.

TABLE II. The parameters and the shadow length.

(a) For $H = 1500$, $h_b = 20$									
H	*1500*	*1500*	*1500*	*1500*	*1500*	*1500*	*1500*	*1500*	*1500*
h_b	20	20	20	20	20	20	20	20	20
l	0	30	60	90	120	150	180	210	240
c	0·00	0·41	0·81	1·22	1·62	2·03	2·43	2·84	3·24
(b) For $H = 1500$, $l = 100$									
H	*1500*	*1500*	*1500*	*1500*	*1500*	*1500*	*1500*	*1500*	*1500*
h_b	0	5	10	15	20	25	30	35	40
l	100	100	100	100	100	100	100	100	100
c	0·00	0·33	0·67	1·01	1·35	1·69	2·04	2·39	2·74
(c) For $h_b = 20$, $l = 100$									
H	*600*	*800*	*1000*	*1200*	*1400*	*1600*	*1800*	*2000*	*2200*
h_b	20	20	20	20	20	20	20	20	20
l	100	100	100	100	100	100	100	100	100
c	3·45	2·56	2·04	1·69	1·45	1·27	1·12	1·01	0·92

Both from equation (1) and Table II, it is apparent that the longer the horizontal distance of the building to the laser origin, the longer the shadow. In other words, the larger the angle of incidence of the laser beam, the longer the shadow length. Certainly, the height of the building is the other positively correlated parameter.

A building located in Erh-Shi-Chang-Li is selected for evaluation with a real data-set. Two lidar strips are selected for the shadow evaluation. The work flow for obtaining the value of each parameter is shown in Fig. 3.

Let the FOV be θ and the width of strip be B, then the flying height H can be computed as

$$H = \frac{B}{2}\cot\frac{\theta}{2}. \tag{2}$$

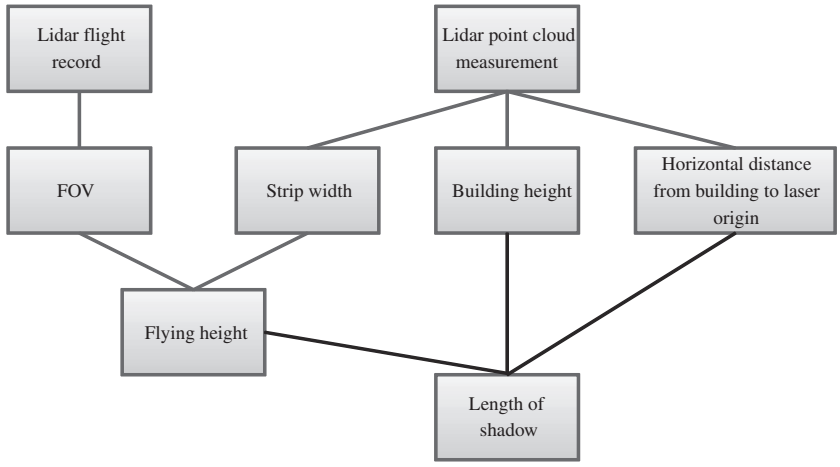

FIG. 3. The sequence of computation.

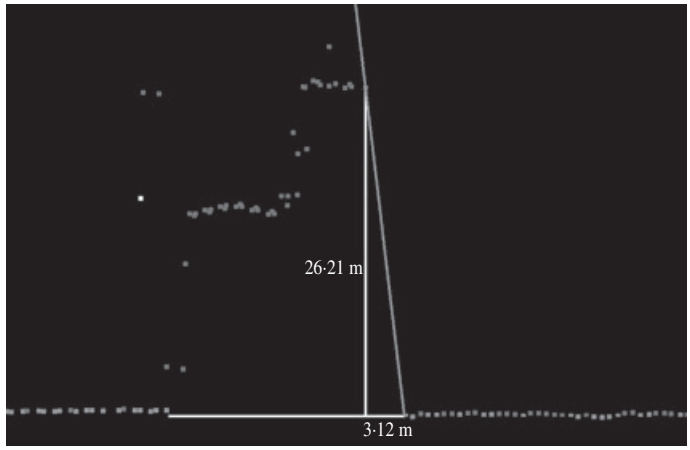

FIG. 4. The profile of a building from the lidar point clouds, strip 27.

The profile of the building across the track in strip 27 is shown in Fig. 4. From equation (2), the following values are obtained:

FOV = 42°
B = 1110 m
H = 1500 m.

From the measurements made in the lidar point clouds

h_b = 26·21 m
l = 196 m.

Following equation (1), the length of shadow c is 3·49 m. Compared with the shadow length of 3·12 m measured from the point clouds, the difference is 0·37 m. This may be caused by the uncertainty in the parameters, such as strip width B, which is the uncertainty introduced to the required flying height.

The profile of the building from the point cloud from strip 28 is shown in Fig. 5. The flying height is also 1500 m. From the point cloud, h_b is 15·5 m. Therefore, l is 462·3 m. The length of shade, c, is 4·83 m. This value is very close to that measured from the point cloud, 4·81 m. The difference is only 0·02 m.

From these two practical examples, the relation presented by equation (1) is confirmed to be valid. The differences between the shadow length measured from the point cloud and that computed may be caused by the uncertainty of parameters. It may also be caused by the uncertainty of both the horizontal and vertical coordinates of lidar points.

OVERLAP DESIGN

Overlapping strips not only enable gaps between strips to be eliminated, but can also reduce the effect of shadows. In this section, the case with a single building is analysed first. Then, the case with two neighbouring buildings is studied. Finally, the significance of the incidence of shadows is examined with a practical data-set.

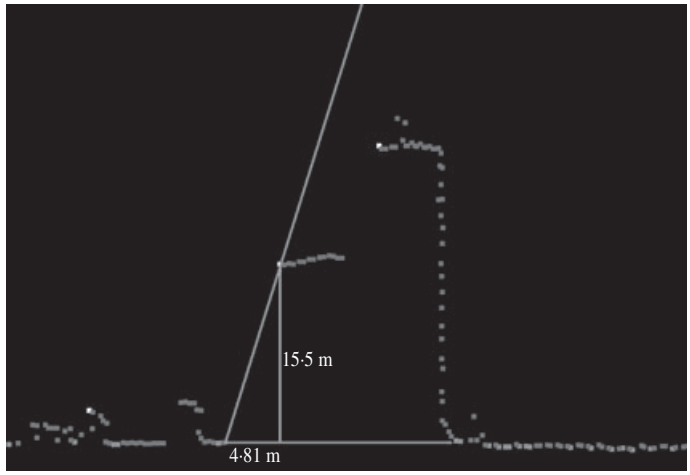

FIG. 5. The profile of a building from the lidar point clouds, strip 28.

Single Building

As shown in Fig. 2, use of a single strip means that shaded areas are inevitable. However, with the overlap from another strip, the shaded area can be eliminated. If the percentage overlap is 50%, almost all shade problems caused by a single building can be eliminated. The current percentage overlap requested by the Ministry of Interior in Taiwan is 40%. The analysis for evaluating the size of the shadow under this situation is as follows.

Let the percentage overlap be x. Then the distance from the strip centre to the non-overlapping area b_n can be computed from

$$b_n = \left(\frac{1}{2} - x\right)B. \tag{3}$$

The tolerance of shadow is related to the required point density. For the density specification of one point per square metre, there will not be any influence if the shade is less than 1 m wide. That is, when $l + 1 < b_n$ and $c > 1$, the shade will affect the completeness of the lidar survey. For most cases of airborne lidar survey in Taiwan, the flying height above the terrain is 1500 m, FOV(θ) equals 42° and percentage overlap (x) is 40%. Therefore, the strip width is 1151·6 m, and the distance from the strip centre to the non-overlap area (b_n) is 115·16 m.

When $l < 115{\cdot}16$ m and $c > 1$ m, the shadow will affect the completeness of data coverage. These two conditions can be rewritten as

TABLE III. h_b and l obtained from equation (4).

l (m)	*20*	*30*	*40*	*50*	*60*	*70*	*80*	*90*	*100*	*114*
h_b (m)	71·43	48·39	36·59	29·41	24·59	21·13	18·52	16·48	14·85	13·04

$$c = \frac{h_b l}{H - h_b} = \frac{h_b l}{1500 - h_b} > 1$$
$$h_b > \frac{1500}{l + 1}. \tag{4}$$

Numerical samples for the relation between h_b and l are listed in Table III. This demonstrates that for a flying height of 1500 m, FOV of 42° and percentage overlap of 40%, shadow lengths can exceed 1 m if there are buildings higher than 13 m. On the other hand, 40% overlap is sufficient if none of the buildings in the non-overlapping area are higher than 13 m.

Two Neighbouring Buildings

The overlap between strips does not eliminate all shade problems. When two buildings are close to each other, the shaded area from two strips may overlap, as shown in Fig. 6.

If the distance between the centres of two neighbouring strips is D, then D can be presented as

$$D = \frac{1}{2}(B_1 + B_2) - X \tag{5}$$

where B_1 and B_2 are the widths of the corresponding strips and X is the width of the overlap.

From Fig. 6, the following relationship can be obtained:

$$c_{12} = l_1 + l_2 + c_1 + c_2 - D. \tag{6}$$

That is, when $l_1 + l_2 + c_1 + c_2 - D > 0$, the overlap of two adjacent strips cannot eliminate the shade problem completely, even if the percentage overlap is 50%.

Two buildings located in Nan-Shih, Hsinchu are taken for the experiment. The buildings are circled in Fig. 7. Two strips, 18 and 19, covered these two buildings. The percentage overlap is 43%. The cross-strip profile of these two buildings is shown in Fig. 8. The measurement of the shade length from the profile of the lidar point cloud is also shown. All three values are measured from the point cloud.

The shade length of these two buildings c_{12} computed from equation (6) is 7·0 m:

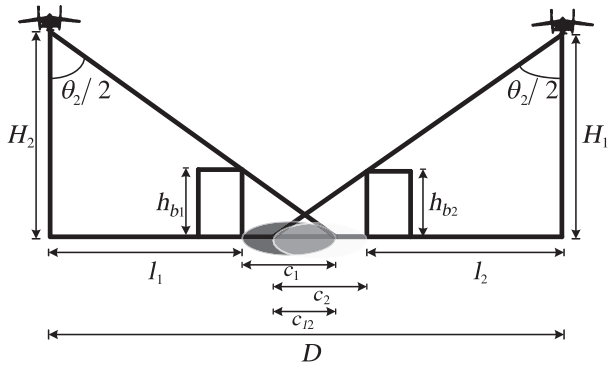

FIG. 6. The shaded area generated from two neighbouring buildings.

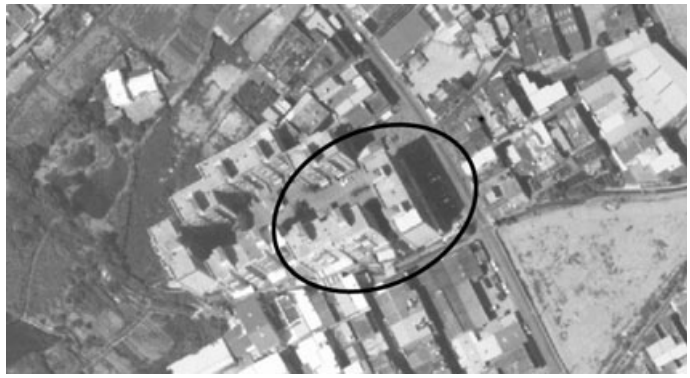

FIG. 7. Aerial photo of buildings in the test area, Nan-Shih, Hsinchu.

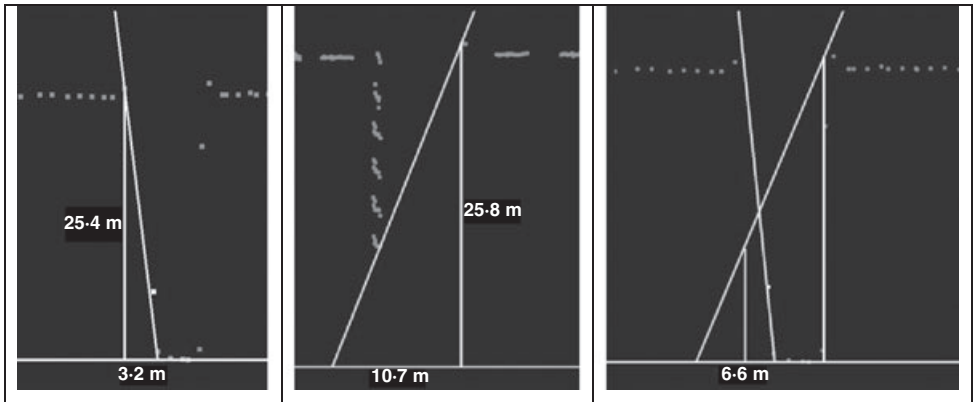

FIG. 8. The profile of buildings from lidar point clouds, Nan-Shih, Hsinchu.

$$c_{12} = l_1 + l_2 + c_1 + c_2 - D = 96{\cdot}5 + 543{\cdot}7 + 3{\cdot}2 + 10{\cdot}7 - 647{\cdot}1 = 7{\cdot}0.$$

From the lidar profile, Fig. 8(c), the measured shade is 6·6 m. The difference is 0·4 m. Despite the difference between the computed and the measured values, it has been demonstrated that the overlap could not completely remove the shadow from neighbouring buildings. Under this situation, reducing the FOV would be an effective solution.

Significance of Incidence of Shadows

After discussing the factors of shade from buildings, the significance of the incidence of laser shadows is examined with the real data-set of Nan-Shih. The flying height is 1500 m above the terrain and the FOV is 42°. The height of the tallest building in this area is 80 m. The data was taken for an area of 2·86 km × 1·12 km. The designed resolution of the final DEM

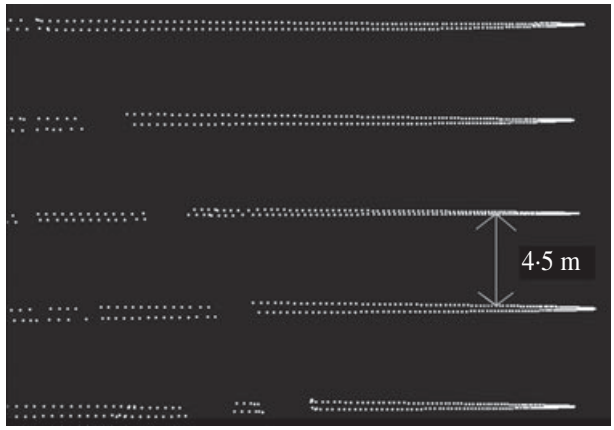

FIG. 9. Point distribution of the right-most portion of strip, Nan-Shih case.

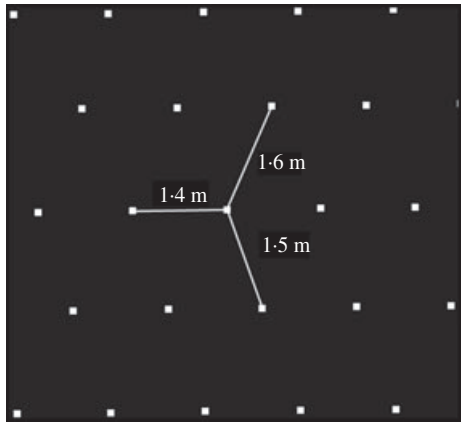

FIG. 10. Point distribution in the central portion of strip, Nan-Shih case.

product is 1 m^2 per cell. The percentage overlap is 42%. The average point density for each single strip is 0·84 points per square metre in this mission. As described with Fig. 1, the point distribution is quite uneven inside the strip. As shown in Fig. 9, the separation between scan lines on the edge is about 4·5 m. The density along the scan line is relatively much higher. In the central area, the point distribution is relatively even. The separation between points is about 1·5 m, as shown in Fig. 10.

Since the cell resolution for the final DEM product is specified as 1 m^2, the evaluation for cells without measured lidar points is performed with the cell size of 1 m × 1 m. However, during the sampling, the radius of influence is set as 1·5 m. That is, starting from the centre of each cell, if there is a point within 1·5 m, the cell is marked as having lidar points. Therefore, for each lidar point, the surrounding 3 × 3 cells will be marked as having lidar points. This is illustrated in Fig. 11. This analysis was performed in the TerraScan environment (Terrasolid, 2005). However, the GEON Point2Grid utility program (Crosby, 2007) would be an ideal tool for performing this task. A good evaluation can be achieved using the point count function

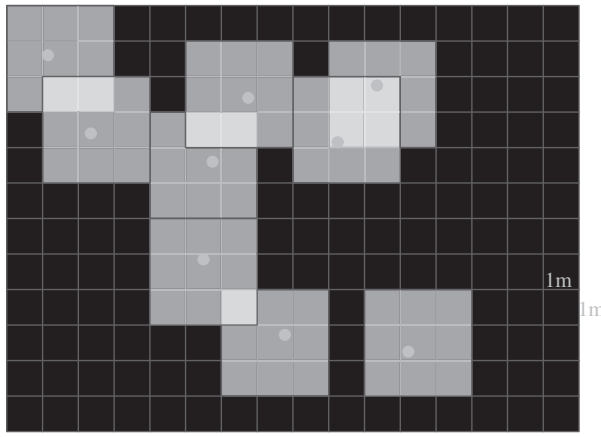

FIG. 11. The sampling scheme in the generation of the final grid.

with a search radius set to 1·5 m. It should be noted that while operated in the TerraScan environment, the city block distance measure was used, that is, the distance was taken as the sum of N and E increments. But in Point2Grid, the Euclidean distance is adopted. The other issue to be settled is the resolution. While the resolution of the final grid can be easily determined with the resolution of the final DEM product, the search radius is somewhat subjective. Crosby (2007) implemented the square root of 2 times the grid resolution as the default value.

Fig. 12(a) is an orthophoto of this area. After analysing the cell without any points, the result is shown in Fig. 12(b) and (c). Fig. 12(b) is the central strip with cells of no lidar points coloured in black. In Fig. 12(c), there is a 42% overlap on both right and left sides. Only the centre 16% is composed of a single strip. As in Fig. 12(b), most cells with no points are caused by the shade of the building. This is effectively reduced with the overlap. It can also be observed that there are more cells with no points in the right and left sides. The number of cells without any points is 6·2% of the total cells.

The improvement with 42% overlap on both sides is shown in Fig. 12(c). The percentage of cells without any points is reduced to 1·1%. The improvement ratio is 82·3%. Comparing Fig. 12(b) and (c), the cells without any points that could not be removed by overlapping strips are mainly bodies of water.

The building shade problem was then evaluated with a data-set from the Taipei Metropolitan area. The building under study was, at the time of writing, the world's highest building already in operation, Taipei 101. The height of this building is 508 m above ground. Because of the shape of the building, the effective height casting a shadow is about 400 m. The lidar data was collected with a Leica ALS50. The set FOV was 19° and the actual FOV ranges between 17·9 and 20·6°. Pulse rate is 54 kHz. The profiles extracted from four strips are shown in Fig. 13. The building shadows computed and measured are listed in Table IV.

CONCLUSIONS

This study investigated the relation between the building height, building location, laser incidence angle, percentage overlap and length of shadow. The following conclusions have been drawn from the present study.

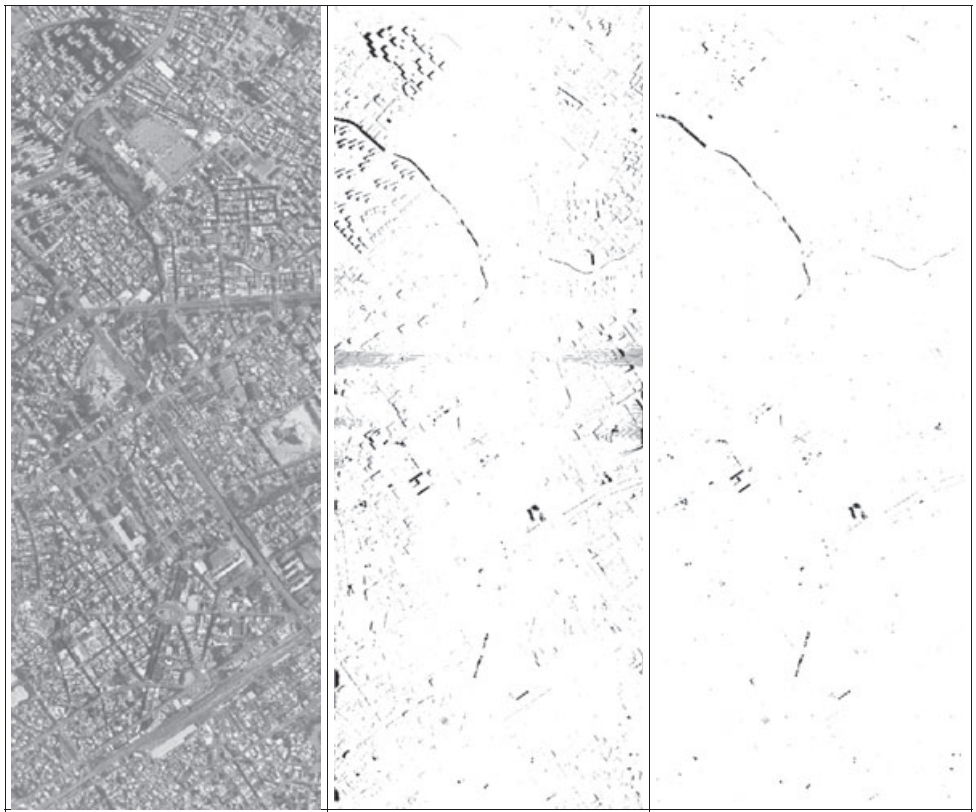

FIG. 12. The influence of strip overlap, Hsinchu City.

The building shadows occur in the cross-flight direction. The length of the shadow is proportionately related to the height of the building, the flying height and the laser incidence angle. For a single building in a single strip, the length of shadow can be computed using $c = (h_b l/(H - h_b))$. For two neighbouring buildings, the shade effect resulting from two overlapping strips can be computed using $c_{12} = l_1 + l_2 + c_1 + c_2 - D$. Both equations are proved to be valid using practical examples.

For the missions designed for 1 m^2 cell resolution, flying 1500 m above the terrain, with FOV of 42°, percentage overlap of 40%, the height of the tallest single building which does not cause shadow problems is 13 m.

The overlap between strips can effectively reduce the building shade problems, but if two buildings are too close to each other, even 50% overlap could not completely eliminate the shadow.

Regarding the error factors, they could be analysed by simply taking the derivatives from equations, such as equation (1). Because the equations are in quite simple format, this will not

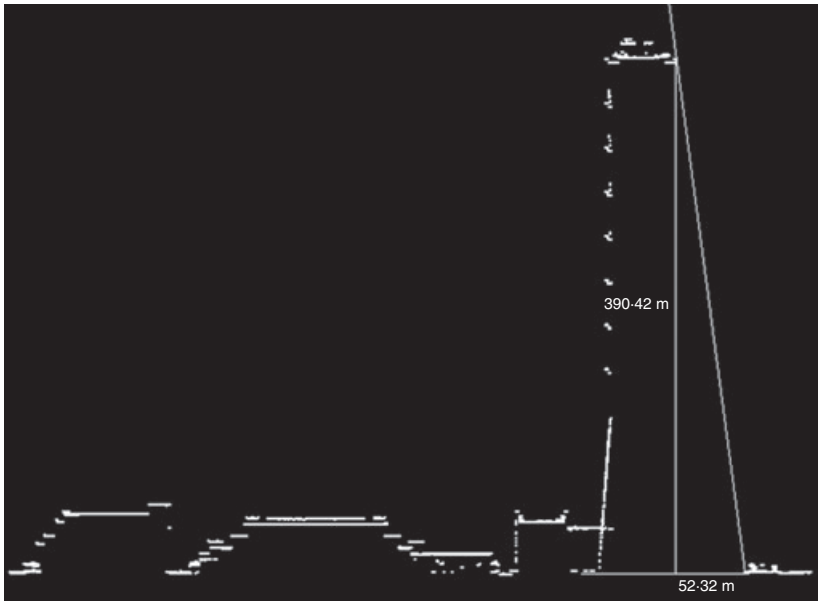

Strip 25
(a)

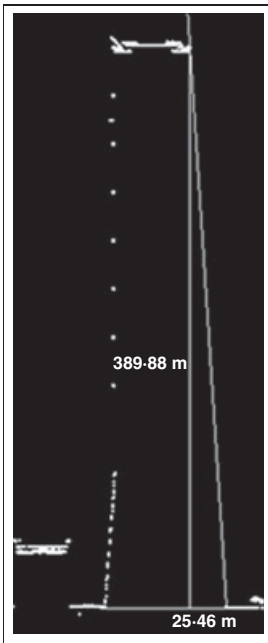

Strip 26
(b)

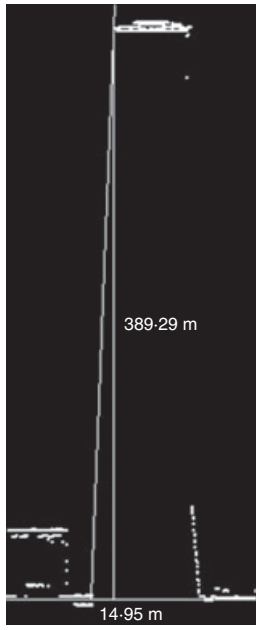

Strip 27
(c)

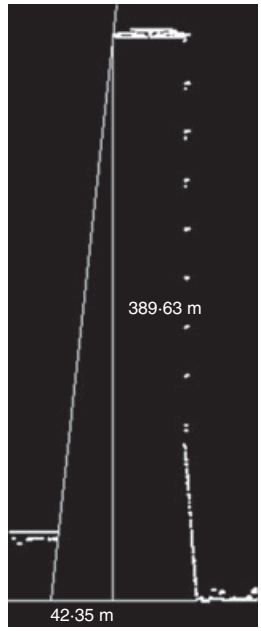

Strip 28
(d)

FIG. 13. The profiles of Taipei 101.

TABLE IV. Measured and computed shadow lengths, Taipei 101.

Strip	*H*	h_b	*l*	*c*	*Measured*
25	1930·30	390·42	202·98	51·46	52·32
26	1944·813	389·88	100·92	25·30	25·46
27	1947·17	389·29	66·34	16·58	14·95
28	2109·14	389·63	184·43	41·79	42·35

be further discussed here. However, from practical experiences, the fore-and-aft tilt of the sensor (that is, around the axis of the aircraft wing, perpendicular to the flight line) during the scanning mission has shown large influence. While the roll angles (around the axis of the line of flight) are effectively compensated by the sensors such as Optech ALTM and Leica ALS, there is no compensation for the tilts. Besides the tilts, another factor which may complicate (but also substantially assist) the overlap design is the use of additional cross-flights at right angles to the main direction of flight.

ACKNOWLEDGEMENTS

The authors wish to thank the National Science Council, Taiwan, Republic of China, for financially supporting this project via grant NSC94-2211-E-009-037. Mr Ken Tsai, National Chiao-Tung University, kindly helped with the data analysis of Taipei 101; his contribution is gratefully acknowledged here. The authors are also grateful to the anonymous reviewers for valuable comments and suggestions which improved the paper.

REFERENCES

ACKERMANN, F., 1999. Airborne laser scanning—present status and future expectations. *ISPRS Journal of Photogrammetry and Remote Sensing*, 54(2/3): 64–67.

BALTSAVIAS, E. P., 1999. Airborne laser scanning: basic relations and formulas. *ISPRS Journal of Photogrammetry and Remote Sensing*, 54(2/3): 199–214.

CROSBY, C., 2007. GEON Point2Grid utility instruction. http://lidar.asu.edu/downloads/GEON_Points2Grid_Instructions.pdf (Accessed: 20th September 2007).

GUENTHER, G. C., THOMAS, R. W. L. and LAROCQUE, P. E., 1996. Design considerations for achieving high accuracy with the SHOALS bathymetric lidar system. *SPIE*, 2694: 54–71.

JAMES, T. D., BARR, S. L. and LANE, S. N., 2006. Automated correction of surface obstruction errors in digital surface models using off-the-shelf image processing. *Photogrammetric Record*, 21(116): 373–397.

LIM, K., TREITZ, P., WULDER, M., ST-ONGE, B. and FLOOD, M., 2003. LIDAR remote sensing of forest structure. *Progress in Physical Geography*, 27(1): 88–106.

NGS, 2004a. *Light detection and ranging (LIDAR) requirements, Scope of Work for Shoreline Mapping under the NOAA Coastal Mapping Program*. National Geodetic Survey, USA. 20 pages.

NGS, 2004b. *Light detection and ranging (LIDAR) requirements, Scope of Work for Airport Surveying under the NOAA Aeronautical Survey Program*. National Geodetic Survey, USA. 26 pages.

SINCLAIR, M., 2005. Hydrographic lidar survey—experiences from Long Island Sound. *U.S. Hydro 2005, The Hydrographic Society of America*. 27 pages. http://www.thsoa.org/hy05/07_4.pdf [Accessed: 20th September 2007].

SOHN, G. and DOWMAN, I. J., 2008. A model-based approach for reconstructing a terrain surface from airborne lidar data. *Photogrammetric Record*, 23(122): 170–193.

TERRASOLID, 2005. *TerraScan User's Guide* (3rd October 2005). Terrasolid, Finland. 169 pages.

VAN AARDT, J. A. N., 2004. *An object-oriented approach to forest volume and aboveground biomass modeling using small-footprint lidar data for segmentation, estimation, and classification*. Ph.D. dissertation, Virginia Polytechnic Institute and State University. 344 pages.

VARGA, T. A. and ASNER, G. P., 2008. Hyperspectral and lidar remote sensing of fire fuels in Hawaii Volcanoes National Park. *Ecological Applications*, 18(3): 613–623.

ZHANG, Y., ZHANG, Z., ZHANG, J. and WU, J., 2005. 3D building modelling with digital map, lidar data and video image sequences. *Photogrammetric Record*, 20(111): 285–302.

Résumé

Les systèmes lidar aéroportés sont équipés d'un mécanisme de balayage qui engendre un couloir de nuages de points pour chaque ligne de vol. Le balayage est perpendiculaire à la direction de vol. La densité du nuage de point est l'un des principaux critères de qualité pour les données acquises par de tels systèmes. La densité des points, l'ombre et le taux de pénétration sont les principaux facteurs à prendre en compte dans la planification d'un vol. Pour des opérations classiques, les missions de vol peuvent être conçues avec des recouvrements compris entre 5 et 50%. De même que le pourcentage de recouvrement, le champ de vue est un autre paramètre important pour la conception du vol. Cette étude propose une méthode d'évaluation pour guider le choix du pourcentage de recouvrement entre couloirs de vol et celui du champ de vue. Les influences du recouvrement et du champ de vue sont aussi démontrées avec des données réelles issues d'un système lidar aéroporté.

Zusammenfassung

Flugzeuggestützte Lidarsysteme sind mit einem Scanmechanismus ausgestattet, der für jeden Flugstreifen eine Punktwolke in Schwadbreite generiert. Die Scanrichtung ist senkrecht zur Flugrichtung. Die Dichte der Punktwolke ist eines der wesentlichen Qualitätsmaße für die erfassten Daten. Punktdichte, Abschattung und Durchdringungsrate sind wesentliche Faktoren, die bei der Flugplanung berücksichtigt werden müssen. Für die Anwendungen in der Praxis werden Überlappungen von 5 bis 50% bei der Flugplanung vorgesehen. Neben der prozentualen Überlappung ist aber auch das Sichtfeld ein weiterer wichtiger Parameter für die Flugplanung. In dieser Studie wird ein Schema zur Bewertung der prozentualen Überlappung zwischen den Flugstreifen und der Auswahl des Sichtfeldes vorgestellt. Deren Einflüsse werden auch an realen Daten eines flugzeuggestützten Lidarsystems demonstriert.

Resumen

Los sistemas lidar aerotransportados van equipados con un mecanismo de escaneado que traza una franja de nubes de puntos en cada pasada de vuelo. El escaneado es perpendicular a la dirección de vuelo. La densidad de la nube de puntos es una de las principales medidas de calidad de los datos obtenidos con estos sistemas. La densidad de puntos, la sombra y la tasa de penetración son los factores más importantes a tener en cuenta en la planificación del vuelo. Por razones operativas las misiones de vuelo se diseñan con recubrimientos que oscilan entre un 5 y un 50%. Aparte del porcentaje de solapamiento, el ángulo de campo es otro parámetro importante a tener en cuenta. Este estudio aporta unos procedimientos de evaluación del recubrimiento entre pasadas y de selección del ángulo de campo. La influencia de estas dos variables se ha determinado con datos de campo obtenidos mediante un sistema lidar aerotransportado.

